Mobility of the Primary Electron-Accepting Plastoquinone Q_A of Photosystem II in a *Synechocystis* sp. PCC 6803 Strain Carrying Mutations in the D2 Protein[†]

Svetlana Ermakova-Gerdes and Wim Vermaas*

Department of Plant Biology and Center for the Study of Early Events in Photosynthesis, Arizona State University, Box 871601, Tempe, Arizona 85287-1601

Received March 20, 1998; Revised Manuscript Received June 18, 1998

ABSTRACT: Upon introduction of random mutations in a region of the *psbDI* gene that encodes the D2 protein in the cyanobacterium *Synechocystis* sp. PCC 6803, an obligate photoheterotrophic mutant was isolated that contained three mutations: V247M, A249T, and M329I. This mutant evolved oxygen in the absence of added electron acceptors, but oxygen evolution was inhibited by micromolar concentrations of several artificial quinones. Complementation analysis showed that the V247M and/or A249T mutations were responsible for this phenotype. Using fluorescence induction and decay measurements, the site of inhibition by the quinones was found to be at the level of the primary electron-accepting quinone in photosystem II, Q_A. Duroquinone inhibited by blocking reduction of Q_A, and in the presence of other quinones such as 2,5-dichloro-*p*-benzoquinone, 2,5-dimethyl-*p*-benzoquinone, and *p*-benzoquinone, Q_A could be reduced but could not efficiently transfer an electron to Q_B. To distinguish the effects of the V247M and A249T mutations, single mutants were created. V247M was photoautotrophic and had an essentially normal phenotype. The A249T mutant, although photoautotrophic, was affected by artificial quinones, but less than the mutant carrying both the V247M and A249T changes. The results indicate a decreased plastoquinone affinity at the Q_A site in the strains carrying a A249T mutation, such that after dark-adaptation a significant percentage of the Q_A sites is empty or is occupied by an artificial quinone. In light, the percentage of photosystem II centers with plastoquinone bound at the Q_A site appears to increase, which may be due in part to an increased affinity of the semiquinone versus that of the quinone at the Q_A site.

Photosystem II (PS II) and the reaction center of purple bacteria have a large number of structural and functional similarities, including a structural homology of the reaction center proteins D1 and D2 of PS II vs the L and M subunits of purple bacteria, and a similarity of electron-transfer reactions at the acceptor side [reviewed in (*1*, *2*)]. However, the properties of the two types of reaction centers also show significant differences. These differences are most pronounced on the electron donor side, and reflect the fundamentally different source of electrons: In PS II, electrons come from water, which is oxidized to yield oxygen [reviewed in (*3*, *4*)], whereas in purple bacteria the oxidized reaction center obtains an electron from a soluble or attached cytochrome *c* [reviewed in (*5*)]. PS II and the purple bacterial reaction center are more similar at the acceptor side, but a number of interesting differences exist. These differences include (a) the position and/or axial ligation of the accessory pigment in PS II predicted to be present between the special pair homologue and pheophytin [see (*6*)], (b) the apparent need of the non-heme iron in PS II (but much less in purple bacteria) for efficient charge separation between P680 and the primary quinone-type electron acceptor Q_A,[1] and for electron transfer between Q_A and the secondary acceptor Q_B (*7*), and (c) the relative difficulty to exchange the plastoquinone Q_A in PS II (*8*). However, in a cyanobacterial mutant lacking a functional non-heme iron, native Q_A was implicated to exchange with artificial quinones (*7*).

The cause of the functional differences between PS II and purple bacteria with respect to Q_A and the non-heme iron is not obvious, but several differences in the composition of the reaction center complexes can be noted. In purple bacteria, the loop between transmembrane helices D and E of the M subunit is seven residues shorter than is expected in the corresponding D2 subunit of PS II, and bacterial reaction centers contain an H subunit that covers part of the acceptor side. PS II is not known to contain an H subunit equivalent, but instead it contains a large number of small subunits with putative membrane-spanning regions. Small, membrane-spanning subunits that are closely associated with the PS II reaction center include cytochrome b_{559}, PS II-H, PS II-I, PS II-L, and PS II-W [reviewed in (*9*)]. PS II-L

[†] This work was supported by the National Science Foundation (MCB 97-28400).

* Corresponding author. Telephone: (602)965-3698. Fax: (602)-965-6899. Email: wim@asu.edu

[1] Abbreviations: BQ, *p*-benzoquinone; DCBQ, 2,5-dichloro-*p*-benzoquinone; DCMU, 3-(3,4-dichlorophenyl)-1,1-dimethylurea; DMBQ, 2,5-dimethyl-*p*-benzoquinone; DQ, tetramethyl-*p*-benzoquinone (duroquinone); F_m, maximal fluorescence yield; F_0, constant fluorescence yield; PS II, photosystem II; Q_A, the first electron-accepting quinone in photosystem II; Q_B, the second electron-accepting quinone in photosystem II.

S0006-2960(98)00659-X CCC: $15.00
Published on Web 07/28/1998

has been shown to influence PS II properties, and results initially were interpreted as PS II-L affecting particularly Q_A affinity and function (*10, 11*). However, more recent data from the same group suggest that PS II-L is not involved in the stabilization of Q_A in its site (*12*). Another factor contributing to different properties of Q_A in PS II and purple bacteria may be the different chemical nature of Q_A in the two types of reaction centers: the conformation of the isoprenyl chain relative to the quinone head is different between PS II, where Q_A is plastoquinone, and purple bacterial reaction centers, where Q_A is ubiquinone or menaquinone (*13*).

It is interesting to note that in PS II the thermodynamic properties of Q_A may be affected by changes on the donor side, indicating a long-distance communication within PS II. Upon depletion of Ca^{2+} but not of Cl^- (both treatments affect the properties of the water-splitting system), the Q_A/Q_A^- midpoint redox potential (E_m) was found to increase by 150 mV (*14, 15*), thus affecting equilibria on the acceptor side of PS II. In further support of long-distance modulation of Q_A properties, in purple bacteria a mutation in E212 of the L subunit, which is about 17 Å away from Q_A, alters the E_m of Q_A/Q_A^- at high pH by about 30 mV (*16*).

Mutant analysis has contributed significantly to the understanding of the role of specific residues in the PS II reaction center complex. Introduction of site-directed mutations at targeted residues has been the predominant strategy to elucidate the role of particular amino acids. The disadvantage of this method is that it is applied only on one or a few targeted residues simultaneously, and therefore is not very appropriate for scanning the function of residues in a larger domain. To remedy this, recently various other methods, such as targeted random mutagenesis and combinatorial mutagenesis, have been applied to PS II (*17, 18*). The targeted random mutagenesis approach involves the introduction of random mutations into a specific part of a gene, followed by screening for functionally impaired mutants (*17*). Here we have used this method to screen for functionally important residues in the C-terminal third of the D2 protein. One of the mutants generated with this screen turned out to be of particular interest in that artificial quinones that usually oxidize the plastoquinone pool and/or accept electrons from PS II were found to be inhibitory to PS II electron transport and appear to bind at the Q_A site. A description of the generation and properties of this and related mutants is provided here.

MATERIALS AND METHODS

Strains and Propagation. Synechocystis sp. PCC 6803 strains used as starting material for this work were the D2-less/CP43-less *psbDIC*$^-$/*psbDII*$^-$ strain (*19*) and the PS I-less/D2-less/CP43-less *psaAB*$^-$/*psbDIC*$^-$/*psbDII*$^-$ strain (*20*). Both strains are obligate (photo)heterotrophs and were propagated at 30 °C in BG11 medium (*21*) in the presence of 5−10 mM glucose. Either a wild-type or a mutant *psbDIC* gene together with a kanamycin-resistance cassette downstream (*19*) was introduced into one of these background strains. In liquid, cultures were either shaken in an Erlenmeyer flask at 120 rpm or bubbled with air. On plates, the BG11/glucose medium was supplemented with 0.3% sodium thiosulfate, 10 mM Tes/NaOH (pH 8.0), 25 μM atrazine, and antibiotics corresponding to resistance markers that had been introduced (25 μg/mL chloramphenicol, 25 μg/mL spectinomycin, 25 μg/mL kanamycin, and 5 μg/mL erythromycin). PS I-containing strains were propagated at 50 μmol of photons m^{-2} s^{-1}; PS I-less strains were grown at 5 μmol of photons m^{-2} s^{-1}.

Targeted Random Mutagenesis of psbDI of Synechocystis sp. PCC 6803. The principles of targeted random mutagenesis have been described in (*22*), and methodologies were similar to those in (*17*). For mutagenesis, the plasmid pDICK carrying *psbDIC* of *Synechocystis* sp. PCC 6803 with a kanamycin-resistance marker downstream (*19*) was used together with a plasmid identical to this except that a 386 bp *Nco*I/*Bsu*36I fragment corresponding to the 3′ end of *psbDI* had been deleted. The latter plasmid will be referred to as deletion plasmid here. The plasmid with wild-type *psbDIC* was cut with *Xho*I, and the deletion plasmid with *Eco*RV. The unique sites in the plasmids for the two enzymes are 4.8 kbp apart from each other. The cut plasmids were mixed in a 1:1 molecular ratio, and were denatured by heating to 90 °C. The mixture was renatured by cooling slowly as described in (*17*) and then treated with 1 or 3 M sodium bisulfite for 4 or 0.3 h, respectively. Sodium bisulfite preferentially deaminates cytosines in single-stranded regions (*23*), and therefore C → U mutations will be introduced in the coding and noncoding strands of the *psbDI* gene between the *Nco*I and *Bsu*36I sites. The sodium bisulfite was removed by dialysis, and the resulting mutagenized DNA was introduced into a uracil−DNA glycosylase-deficient strain of *E. coli*. Plasmids were allowed to segregate in liquid, and small aliquots were plated out 2 h after transformation. Colonies carrying intact *psbDIC* (rather than those carrying a deletion) were selected making use of the fact that expression of intact *psbDIC* slows down *E. coli* growth: small transformant colonies were selected, and these were all found to carry plasmids with full-length *psbDIC*. These plasmids were used to transform the *psbDIC*$^-$/*psbDII*$^-$ strain of *Synechocystis* sp. PCC 6803, and transformants with impaired PS II properties were identified by replica plating on plates with and without 5 mM glucose.

Thylakoid Preparation, SDS−PAGE, and Western Blotting. The procedures for thylakoid preparation, SDS−PAGE, protein transfer to the poly(vinylidene difluoride) membrane, and immunohybridization with D2 antiserum have been described (*24*). Protein quatitation was performed using the BCA (bicinchoninic acid) Protein Assay Kit (Pierce, Rockford, IL) according to the instructions of the manufacturer.

Electron Transport Measurements. Oxygen evolution measurements were carried out with a Gilson oxygraph, Model KM, at 25 °C. Measurements were carried out in the absence of added electron acceptors unless indicated otherwise. Sufficient endogenous electron acceptors are present in intact cells to support oxygen evolution for several minutes.

Fluorescence Measurements. Fluorescence induction and decay of the chlorophyll *a* fluorescence yield after a flash were measured using a Walz PAM fluorometer. The light intensity of the measuring light was kept low, particularly in the presence of DCMU [3-(3,4-dichlorophenyl)-1,1-dimethylurea], to avoid a possible actinic effect of the measuring light. Decay of the variable fluorescence was

measured after a microsecond flash generated by a Xe flash lamp.

Herbicide Binding Analysis. Specific binding of ^{14}C-DCMU to intact cells was used to quantify the amount of PS II on a chlorophyll basis following a protocol similar to that in (*25*). For this purpose, 1 mL aliquots of cells (at a concentration corresponding to 25−50 μg/mL chlorophyll) suspended in 25 mM Hepes/NaOH (pH 7.5) were incubated for 10 min in low light with several different nanomolar concentrations of ^{14}C-DCMU in the presence and absence of 20 μM atrazine, a competitive inhibitor of DCMU binding. The amount of specific DCMU binding at a particular concentration of free DCMU was determined by centrifugation of the cells, counting the amount of radioactivity in 0.8 mL of the supernatant, and calculating the amount of bound DCMU, followed by subtraction of the amount of DCMU bound in the presence of atrazine (unspecific binding) from the amount of DCMU bound in the absence of atrazine. The free DCMU concentration was plotted against the amount of bound DCMU in a double-reciprocal plot, providing information regarding the number of DCMU binding sites and the DCMU affinity.

RESULTS

Mutant Generation. Several obligate photoheterotrophic *Synechocystis* sp. PCC 6803 mutants were isolated after targeted random mutagenesis of *psbDI* using sodium bisulfite *in vitro*. One of these mutants had mutations leading to three changes in the D2 protein: V247M/A249T/M329I. This mutant has been named D2R8 (designating that it is random mutant 8 in the D2 protein). Residues 247 and 249 are expected to be located in a loop region on the cytoplasmic side of the thylakoid membrane between the fourth and fifth membrane-spanning helix. Residue 329 is expected to be at the lumenal side, beyond the fifth and last transmembrane span.

To distinguish whether mutations in residues 247 and/or 249 or in residue 329 gave rise to the obligate photoheterotrophic phenotype, the D2R8 mutant was transformed with 330 or 236 bp wild-type *psbDI* fragments that covered either codons 247 and 249 or codon 329, respectively. Only transformation with the 330 bp *Nco*I/*Taq*I *Synechocystis* sp. PCC 6803 *psb*DI wild-type gene fragment covering D2 codons 247 and 249 gave photoautotrophic colonies that propagated with normal growth rates, indicating that the reason for the mutant's obligate photoheterotrophic phenotype is located at residue 247 and/or 249. Therefore, the focus of this paper will be on these two residues.

Photosystem II Electron Transport. Although the obligate photoheterotrophic phenotype of the D2R8 mutant would suggest that overall PS II electron transport for extended periods of time was insufficient for photoautotrophic growth, in the absence of artificial electron acceptors this mutant was able to evolve oxygen at rates that were about 30% of those in the control strain (Table 1). The control strain was generated by transformation of the *psbDIC*$^-$/*psbDII*$^-$ strain with the pDICK plasmid (*19*), carrying wild-type *psbDIC* and a kanamycin-resistance marker downstream. However, interestingly, the addition of an artificial quinone such as 2,5-dichloro-*p*-benzoquinone (DCBQ), 2,5-dimethyl-*p*-benzoquinone (DMBQ), tetramethyl-*p*-benzoquinone (duroquinone; DQ), or *p*-benzoquinone (BQ) at concentrations below 0.3 mM inhibited the rate of oxygen evolution in the D2R8 mutant (Table 2 and Figure 1). Particularly DQ was found to have a very prominent inhibitory effect at micromolar concentrations. This quinone was capable of total inhibition of oxygen evolution, whereas addition of other quinones led only to partial inhibition of electron transfer at the concentrations assayed (Table 2).

Table 1: Rates of Photoautotrophic Growth and Electron Transport, Number of DCMU Binding Sites on a per-Chlorophyll Basis, and DCMU Affinity in the Control Strain and the D2R8, V247M, and A249T Mutants

strain	autotrophic doubling time (h)	O_2 evolution [μmol of O_2 (mg of Chl)$^{-1}$ h^{-1}]	Chl/DCMU ratio	Chl/PS II ratio (% of control)	K_D, DCMU (nM)
control	12	325	550 ± 30	100	17 ± 1
D2R8	−	100	3700 ± 600	15	66 ± 11
V247M	18	260	660 ± 70	83	12 ± 3
A249T	40	150	1980 ± 190	28	22 ± 3

Table 2: Quinone Concentrations That Cause 50% Inhibition of Oxygen Evolution (I_{50}), and Levels of Inhibition of Oxygen Evolution Achieved upon Addition of 300 μM Quinone in the D2R8 and A249T Mutants and in the Control Strain

quinone added	I_{50} (μM)			inhibition (%) at 300 μM		
	D2R8	A249T	control	D2R8	A249T	control
DQ	2	18	na[c]	100	93	46
DCBQ	37	350	*	91	49	0
DMBQ	135	*[a]	*	80	0	0
BQ	200	nd[b]	*	80	nd	0

[a] *: no inhibition in the concentration range tested (up to 300 μM). [b] nd: not determined. [c] na: 50% inhibition could not be achieved.

To determine which of the mutations at these two residues contributed most to the obligate photoheterotrophic phenotype and to the observed sensitivity of PS II electron transfer to artificial quinones, two single mutants, V247M and A249T, were generated by means of site-directed mutagenesis and introduced into the *psbDIC*$^-$/*psbDII*$^-$ strain of *Synechocystis* sp. PCC 6803. As indicated in Table 1, the photoautotrophic growth rate of V247M is 70% of that of the control whereas the single mutant A249T is capable only of very slow photoautotrophic growth at a rate that is 30% of that of the control. As expected, under photomixotrophic conditions (in the presence of 5 mM glucose), the mutants can be propagated with essentially the same doubling time as the control strain (data not shown). These data indicate that the A249T mutation has a more prominent effect than the V247M one, but that the double mutation has a larger effect than either of the two single mutations: the original mutant could not grow photoautotrophically even when provided with the wild-type DNA covering codon 329, indicating that the phenotype of the V247M/A249T double mutant was obligate photoheterotrophic.

An inhibitory effect of exogenous quinones was also observed in A249T, although in this mutant the effect was less pronounced than in D2R8 (Table 2 and Figure 1). The properties of V247M were found to be similar to those of the control strain, in which no inhibition of PS II function by DCBQ and DMBQ at concentrations of up to 0.4 mM was detected (data not shown). This indicates that indeed

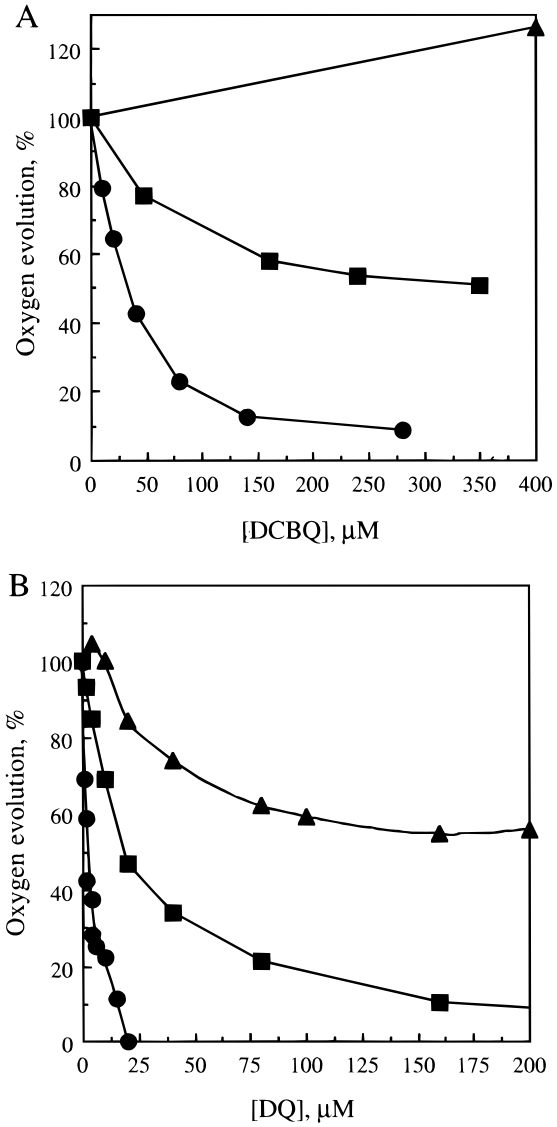

FIGURE 1: Inhibition of oxygen evolution by DCBQ (A) and DQ (B) in the D2R8 (●) and A249T (■) mutants and in the control strain (▲). Oxygen evolution was measured at saturating light intensity in the presence of 0.5 mM $K_3Fe(CN)_6$ to keep quinones oxidized.

mostly the A249T mutation is responsible for the observed quinone effects.

For other quinones that were tested some inhibition of electron transport was observed in the control strain at high quinone concentrations, but in all cases the I_{50} value, which is the quinone concentration that needs to be added for 50% inhibition of electron transport, was found to be several times higher for the control strain than for the D2R8 and A249T mutants (Table 2). Interestingly, as is shown in Figure 1, full inhibition of oxygen evolution is not achieved by all artificial quinones, even not in D2R8; this suggests that some electron transport can still occur in this mutant in the presence of saturating concentrations of several artificial quinones.

PS II Quantitation and DCMU Affinity. To quantify the number of PS II centers on a chlorophyll basis and to determine whether major changes had occurred in the Q_B/herbicide binding niche (to which also some quinones are known to bind) in the mutants and in the control strain, binding assays were performed with different concentrations of radiolabeled DCMU (*25*). This measurement provides information both on the number of chlorophylls per DCMU binding site and on the DCMU dissociation constant. The results are summarized in Table 1. The amount of PS II centers in the D2R8 mutant and in A249T was found to be 12−18% and 25−30%, respectively, of that of the control strain. V247M had about 80% of the wild-type amount of PS II complexes in its thylakoid membranes on a per-chlorophyll basis. These percentages are similar to the relative rates of oxygen evolution in the various mutants (Table 1), indicating that the remaining PS II centers in the mutants appear to function normally in continuous light.

Interestingly, the dissociation constant for DCMU in the D2R8 mutant was increased 4-fold as compared to in the control strain, whereas the DCMU affinity of the A249T and V247M mutants was essentially normal (Table 1). As expected, the decreased affinity of PS II centers for DCMU in D2R8 led to a decreased level of DCMU sensitivity in this strain: the concentration of this herbicide required for 50% inhibition of oxygen evolution in intact cells at saturating light intensity was 175 nM in the D2R8 mutant whereas it was 40 nM in wild-type cells (data not shown). This extends earlier observations (*26*) that mutations in the D2 protein can modulate the properties of the Q_B niche.

Mutants in a PS I-less Background Strain. For further characterization by means of fluorescence, we intended to introduce the D2R8, A249T, and V247M mutations into a PS I-less strain, as in such strains the variable fluorescence is much larger (*27*). However, introduction of these mutations into a PS I-less strain that lacked *psbDIC* and *psbDII* (*20*) led to the surprising observation that both the D2R8 and the A249T mutant in a PS I-less background did not accumulate a measurable amount of PS II: (1) immunodetection of the D2 protein in the D2R8 mutant and in the control strain (both in PS I-less backgrounds) indicated that the amount of D2 was decreased about 25-fold in the D2R8 mutant as compared to in the control (Figure 2); (2) the chlorophyll/OD_{730} ratio of the D2R8 and A249T strains in a PS I-less background was close to that of the *psbDIC*$^-$/*psbDII*$^-$/PS I-less mutant and about 3-fold lower than that present in a PS I-less strain with normal PS II; (3) no oxygen evolution was detected in the D2R8/PS I-less and A249T/PS I-less strains in the presence of small concentrations of artificial quinones; and (4) the 77 K fluorescence emission spectrum of these strains showed a peak at 684 nm but no 695 nm emission shoulder or peak was observed (data not shown). Particularly the observation that the A249T mutant did not accumulate PS II in a PS I-less background is surprising, because in a PS I-containing background the A249T mutant was photoautotrophic, even though it grew slowly under these conditions. The reason for the lack of apparent PS II synthesis and/or stability in the A249T mutants in a PS I-less background is not obvious, but may be related to a difference in the redox state of the cells in PS I-containing and PS I-less strains. The V247M mutant in a PS I-less background assembled a fairly normal amount of PS II as determined by oxygen evolution rates and the amount of chlorophyll on a per-cell basis (data not shown). As the A249T and D2R8 mutants were not found to contain a measurable amount of PS II when in a PS I-less background, subsequent experiments on these mutants were carried out in a PS I-containing background strain.

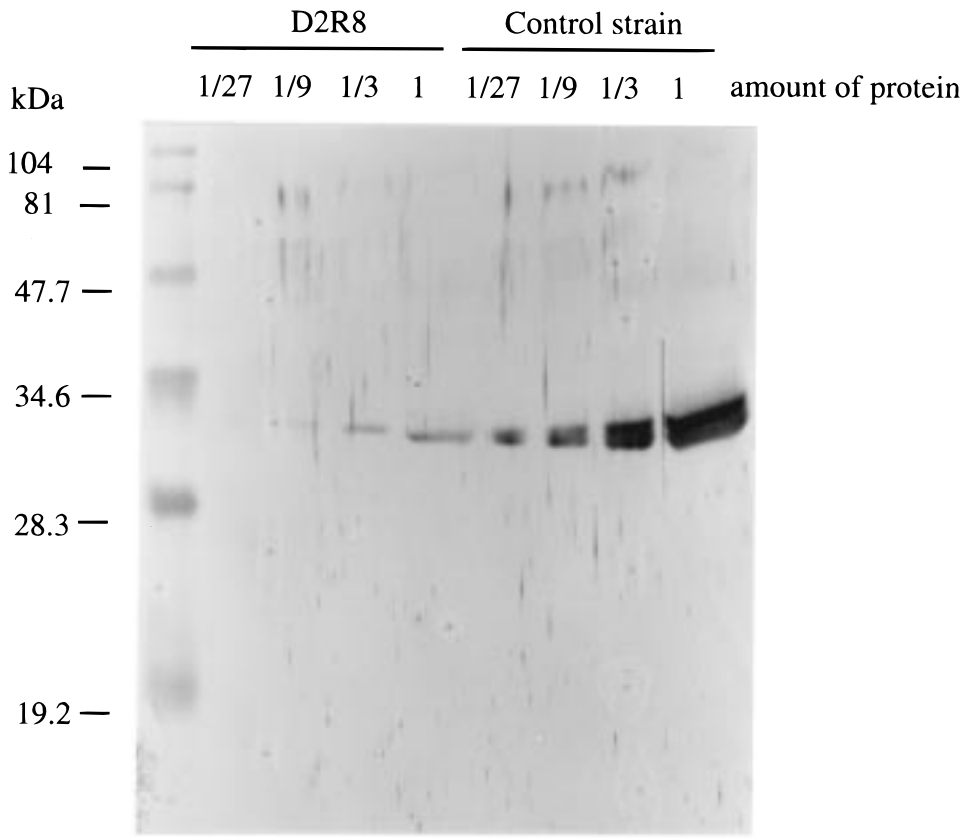

FIGURE 2: D2 quantitation by Western blotting of thylakoid proteins from the D2R8 mutant in a PS I-less background (left four lanes) and from the PS I-less control strain (right four lanes), immunodecorated with D2 antibodies. The amount of thylakoid proteins for the two strains was identical in corresponding lanes and corresponded to 25 μg (according to the bicinchoninic acid protein assay) in lanes labeled "1". The amounts of protein in the other lanes were serial dilutions as indicated. The position of the molecular mass standards (kDa) has been indicated as well.

Fluorescence Induction. Fluorescence induction kinetics in the D2R8 and A249T mutants were unusual (Figure 3). As expected, in the control strain without additions, a rise in the chlorophyll fluorescence yield was observed until a maximum was reached after about 600 ms after the start of illumination (Figure 3A). In contrast, a much smaller and slower rise was observed in the A249T mutant (Figure 3B), and no rapid induction of variable fluorescence was observed in the D2R8 mutant under the same conditions (Figure 3C); instead, a very slow increase in the fluorescence yield was seen upon illumination in D2R8 (Figure 3D), and upon turning off the light after several seconds of illumination, only a small fraction of the fluorescence intensity decreased rapidly (Figure 3D).

In the presence of DCMU, only a single electron can be transported up to Q_A, and in the control strain fluorescence induction is rapid and complete. The fluorescence level attained is much higher than seen in the absence of DCMU, indicating that in the absence of the inhibitor Q_A is only partly reduced in the control strain in the light (Figure 3A). However, fluorescence induction of the D2R8 mutant in the presence of DCMU was very slow but was faster than seen in its absence (Figure 3C,D). The A249T mutant showed an intermediate fluorescence induction curve in the presence of DCMU, with part (about half) of the induction being very fast whereas the remaining part was much slower. However, this slow phase was faster than was seen in D2R8 (Figure 3B).

Interestingly, a rapid induction of variable fluorescence in the D2R8 mutant was restored by addition of 160 μM DCBQ in the presence of DCMU (Figure 3C,D). DMBQ and BQ had a similar effect (Figure 4). However, rapid fluorescence induction could not be restored in the D2R8 mutant with DQ and DCMU (Figure 4). This effect of DQ is not due simply to efficient fluorescence quenching by this quinone. The same concentration of DQ quenches only 15% of the variable fluorescence in the control strain.

In the A249T mutant, addition of 160 μM DCBQ in the presence of DCMU led to a rapid and full fluorescence induction, and the slow phase of induction was no longer observed (Figure 3B). Under these conditions, the maximum yield of variable fluorescence in the mutants $[(F_m - F_0)/F_0 = 0.09$ and 0.15 in the D2R8 and A249T mutants, respectively] in comparison with that of the wild type $[(F_m - F_0)/F_0 = 0.54]$ was close to the amount expected from the PS II content of the mutant as determined by the ^{14}C-DCMU binding assay (see Table 1).

The results obtained thus far are interpreted most simply by the hypothesis that in the D2R8 mutant after incubation in darkness most or all PQ is absent from the Q_A site and thus cannot be reduced by PS II electrons, and that many artificial quinones except DQ can functionally replace PQ at the Q_A site but cannot efficiently transfer electrons to Q_B, thus causing an overall inhibition of electron transport. DQ would be able to bind to the Q_A site but not be reduced. As in continuous light oxygen evolution occurs in the D2R8

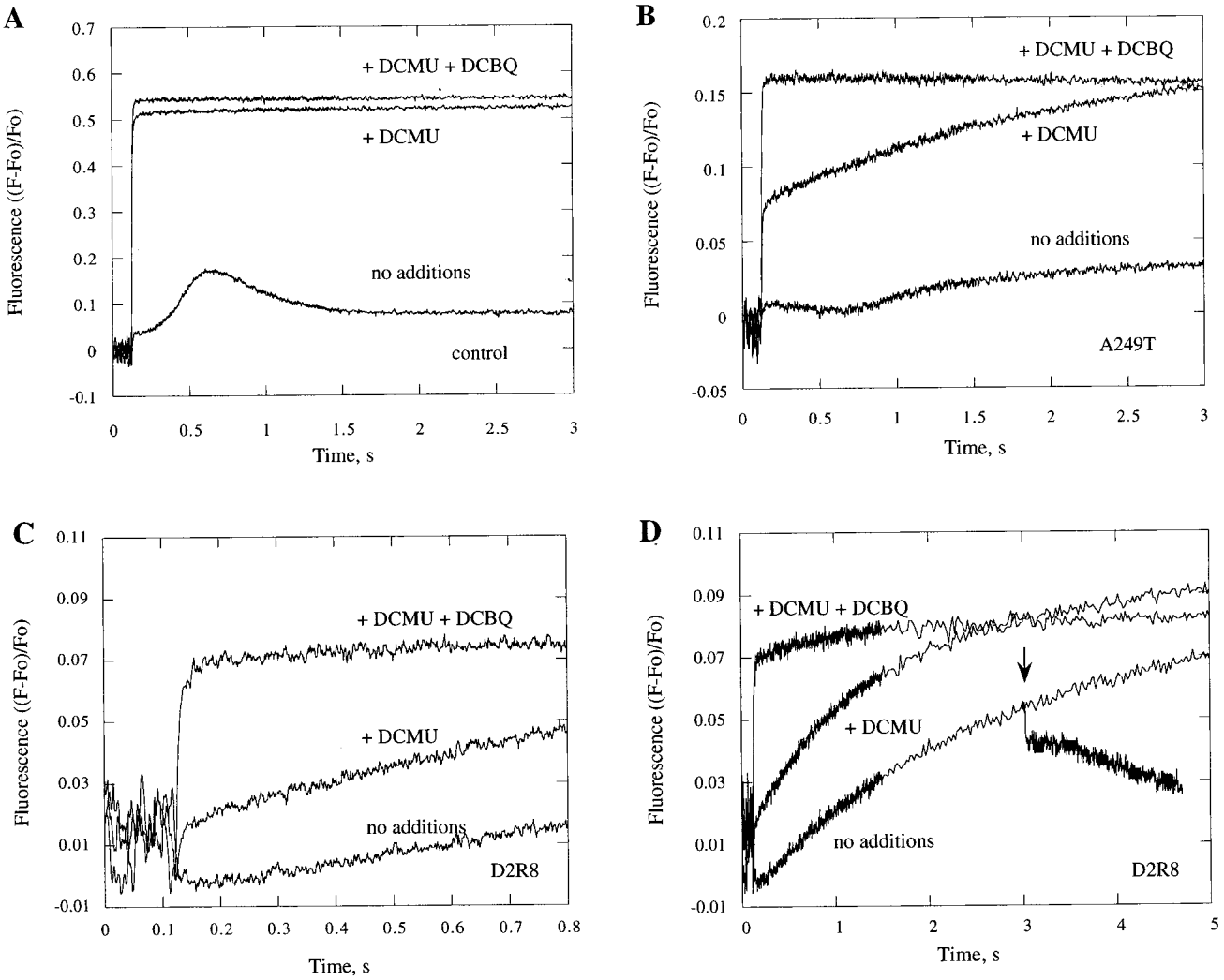

FIGURE 3: Fluorescence induction in intact cells of the control strain (A) and in the A249T (B) and D2R8 (C, D) mutants in the absence of any additions (lower traces) and in the presence of 100 μM DCMU and/or 160 μM DCBQ as indicated. In panel D, the trace without additions is split into two after 3 s illumination (indicated by an arrow): the upper trace represents continued illumination, and the lower trace reflects the fluorescence yield when the actinic light is turned off. Panels C and D have been recorded on different time scales. Constant fluorescence (F_0) has been subtracted, and variable fluorescence yields have been normalized to F_0. The chlorophyll concentration in all samples was 10 μg/mL.

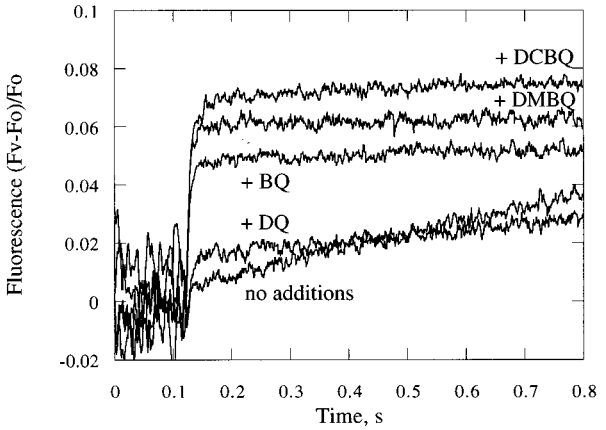

FIGURE 4: Fluorescence induction of D2R8 in the presence of 100 μM DCMU. Artificial quinones (160 μM) were added as indicated. Constant fluorescence (F_0) has been subtracted, and variable fluorescence yields have been normalized to F_0. The chlorophyll concentration in all samples was 10 μg/mL.

mutant in the absence of added quinone, in the light PQ seems to remain in the Q_A site once functionally bound. The A249T mutant has most of the features of D2R8, but A249T appears to retain functional binding of PQ at the Q_A site in about half of the centers in darkness (Figure 3B). In the following sections, experiments were performed to determine the validity of our reasoning that PQ at the Q_A site is mobile in the D2R8 strain and can be replaced by artificial quinones.

Herbicide Binding in the Presence of Added Quinones. One consequence of the hypothesis that exogenous quinones inhibit the D2R8 mutant by binding to the Q_A site rather than to the Q_B site [where artificial quinones are known to bind with low affinity in wild-type systems (*28, 29*)] is that DCMU binding, which occurs at the Q_B site, should not be greatly affected by inhibiting quinones. To test this, the effect of addition of 160 μM DQ, which has an I_{50} of 2 μM in inhibiting PS II electron transfer in the D2R8 mutant (see Table 2) and is known to not bind tightly to the Q_B site in wild-type systems (*28, 29*), was probed on binding of ^{14}C-DCMU to cells of this mutant. DCMU binds at the Q_B/herbicide binding niche, and herbicides and artificial quinones show more or less competitive binding characteristics to the Q_B site. Whereas atrazine addition caused full DCMU displacement, addition of 160 μM DQ, which fully inhibited

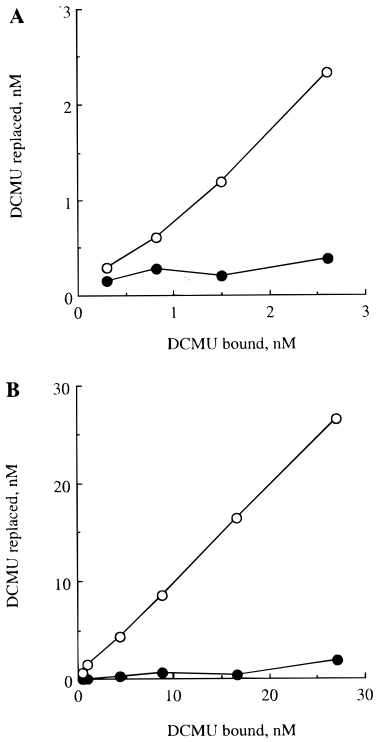

FIGURE 5: Replacement of bound, ^{14}C-labeled DCMU from intact cells by addition of 100 μM atrazine (○) and 160 μM DQ (●) in the D2R8 mutant (A) and in the control strain (B). The chlorophyll concentration in the samples was 50 μg/mL.

oxygen evolution, did not significantly alter DCMU binding in the V247M/A249T mutant (Figure 5A). The small DQ-induced displacement that is seen is similar to that in the control strain (Figure 5B; note the difference in scales). This implies that the site of DQ inhibition of oxygen evolution in the D2R8 mutant is not at the Q_B niche.

Kinetics of Q_A^- Oxidation by Q_B. In the absence of artificial quinones, the amplitude of variable fluorescence upon single-turnover flashes in the D2R8 mutant was found to be less than 10% of that in the presence of artificial quinones and 100 μM DCMU. This is as would be expected from the results shown in Figure 3C,D. In view of the small amplitude of the signal, a reliable estimation of the Q_A^- decay kinetics after the flash in the absence of inhibitors could not be obtained, but appeared to be about 800 μs (Figure 6). Upon addition of 160 μM DCBQ, only a minor fast phase remained, and a large part of Q_A^- generated by the flash remained stable for more than 20 ms. In addition, a 50% increase in signal amplitude was seen upon addition of DCBQ.

Q_A^- Oxidation by Charge Recombination. In addition to Q_A^- oxidation by Q_B, Q_A^- oxidation in the presence of DCMU, which reflects charge recombination with the PS II donor side, was determined. In Figure 7A, the amount of variable fluorescence after a flash was monitored as a function of time. In the presence of DCMU, the Q_A^- decay kinetics in D2R8 were slower than in the wild type. According to the results presented in Figure 7B, the decay kinetics became significantly faster in the presence of exogenous quinones. In some cases the fluorescence decay kinetics were clearly biphasic, and a deconvolution of the rates of Q_A^- oxidation observed in the presence of DCMU and DCBQ or DMBQ is provided in Table 3. In the D2R8

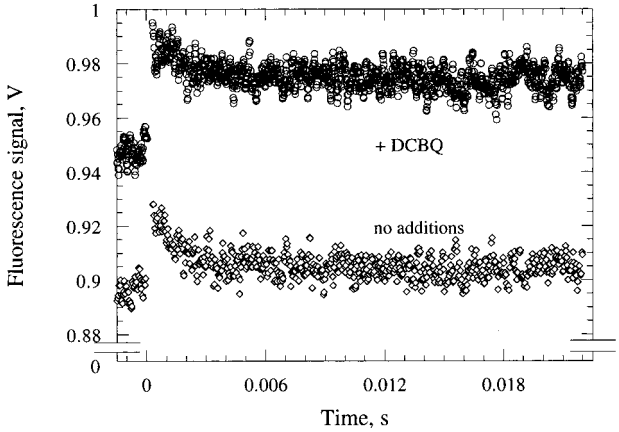

FIGURE 6: Decay of flash-induced variable fluorescence in the D2R8 mutant in the presence (top) and absence (bottom) of 160 μM DCBQ. A subsaturating Xe flash was given at time 0. The fluorescence yield was measured in time using weak, nonactinic flashes. Traces represent the average of 8 experiments.

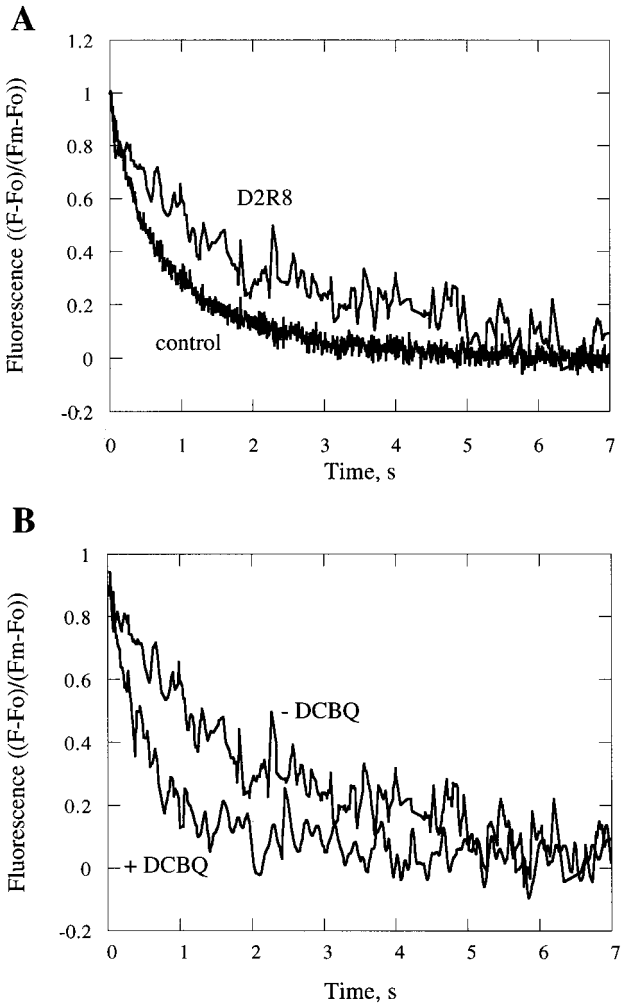

FIGURE 7: (A) Decay of flash-induced variable fluorescence in intact cells of the control strain and of the D2R8 mutant in the presence of 100 μM DCMU. The maximal variable fluorescence yield was normalized to 1 for both strains to facilitate comparison. (B) Decay of flash-induced variable fluorescence in intact cells of the D2R8 mutant in the presence of 100 μM DCMU and in the presence or absence of 210 μM DCBQ. The chlorophyll concentration in the samples was 10 μg/mL.

mutant, addition of artificial quinone sped up the charge recombination. As expected, quinone addition did not have

Table 3: Kinetics of Q_A^- Oxidation in the Presence of 70 μM DCMU and 240 μM Quinone (as Indicated) in the D2R8 Mutant and the Control Strain[a]

strain	quinone added	A_1	$(t_{1/2})_1$ (s)	A_2	$(t_{1/2})_2$ (s)
D2R8	none	–	–	100	1.59
	DCBQ	49	0.20	51	1.54
	DMBQ	60	0.46	40	2.63
control	none	47	0.18	53	0.97
	DCBQ	52	0.20	48	0.95
	DMBQ	52	0.19	48	1.09

[a] Chlorophyll fluorescence decay traces were deconvoluted assuming the presence of two exponential components; if a one-component deconvolution provided an equally good fit, the second component was omitted. A_1 and A_2 represent the amplitudes of the two phases (normalized to give a sum of 100); $(t_{1/2})_1$ and $(t_{1/2})_2$ are the corresponding decay half-times.

a significant effect on Q_A^- oxidation kinetics in the presence of DCMU in the control strain (Table 3).

Oxygen Evolution as a Function of Light Intensity. To determine the quantum yield of PS II in the D2R8 mutant as compared to the control strain, oxygen evolution was measured at different light intensities. Excitation at wavelengths greater than 665 nm (mainly absorbed by chlorophyll) was used in order to overcome possible differences in the amount of light transferred to PS II reaction centers by phycobilisomes in D2R8 and the control strain, since the phycobilisome/PS II ratio is significantly higher in the mutant: upon a mutation-induced decrease of the amount of PS II per cell, the number of phycobilisomes remains fairly constant [for example, see (*30*)]. The D2R8 strain needed a 2-fold higher light intensity in order to obtain half the saturation rate as compared to the control strain (800 vs 380 μmol of photons m^{-2} s^{-1}) (data not shown). This suggests that the quantum yield of charge separation in continuous light was decreased by a factor of 2 in the mutant if no artificial quinones had been added.

DISCUSSION

Functional complementation assays indicated that in the triple mutant V247M/A249T/M329I the V247M/A249T mutation combination was responsible for the obligate photoheterotrophic phenotype observed. The fact that M329I does not appreciably contribute to the phenotype is not surprising in that single-residue replacements in the C-terminal lumenal domain of the D2 protein have not yielded a phenotypic effect [reviewed in (*31*)].

The Ala249 and Val247 Residues. According to the structure of the reaction center from purple bacteria, the two oxygens of the Q_A ring are hydrogen-bonded to the side chain of a His or a Thr and to the peptide nitrogen of an Ala group in the M subunit (*32*−*34*). A similar arrangement is assumed for Q_A in D2, even though direct experimental data on the position of Q_A in D2 are limited and are not necessarily in agreement with each other regarding whether His hydrogen bonds with a Q_A oxygen or not (*35*, *36*). The Ala in purple bacteria that has a peptide nitrogen hydrogen-bond to Q_A, residue 258 of the M subunit, does not appear to be homologous to Ala249 of D2: if Trp250 of the M subunit, which is located between Pheo and Q_A, is homologous to Trp253 of D2, which has been shown to be important for PS II stability (*37*), then a simple alignment extension would suggest that the analogue of Ala258 of the M subunit is either Phe261 or Ala260 of D2. Ala249 of D2 therefore is unlikely to hydrogen-bond an oxygen of Q_A. Instead, based on a simple alignment rooted at Trp250 (M subunit)/Trp253 (D2), Ala249 of D2 is expected to be homologous to Ala246 of the M subunit, which is about 4 Å from Q_A in purple bacteria (*34*).

Ala249 of D2 may have its counterpart in Ala251 of the D1 protein. This Ala residue in D1 is known to be part of the herbicide binding niche because a mutation to Val affects the sensitivity to herbicides (*38*, *39*). Mutation of Ala251 of the D1 protein to a variety of other residues in *Chlamydomonas reinhardtii* leads to a loss of photoautotrophic capacity and to a decrease in D1 stability (*40*).

Mutation of Val247 of the D2 protein has an additional impact on Q_A function. In the D1 protein, a Val residue is also present two residues toward the N-terminus from Ala251, the residue that is likely to be homologous to Ala249 in D2. No Val249 mutations in D1 have been reported yet, but this residue is the primary target of an azido-labeled herbicide analogue, azidoioxynil (*41*), and therefore is likely to be part of the Q_B/herbicide binding niche. The Val247 residue of D2 is assumed to be near the N-terminal end of the putative *de* helix (*42*), and a mutation in this residue may affect the length or orientation of this helix.

Properties of the D2R8 Mutant. A very interesting feature of the D2R8 mutant is that PS II electron transport is inhibited by artificial quinones that usually are used as electron acceptors. Subsequent analysis showed that the A249T mutation is the main contributor to the phenotype of obligate photoheterotrophic growth and sensitivity to artificial quinones, but neither the A249T nor the V247M mutation causes as striking a phenotype as is found in the D2R8 mutant.

The interpretation we have developed on the basis of the results presented in this paper is that in the D2R8 mutant PQ at the Q_A site is mobile and can be replaced by other quinones. A similar interpretation was used to explain experimental results obtained with a mutant in which His268 of the D2 protein, presumably a ligand to the non-heme iron, had been mutated to Gln (*7*). Unlike the situation with the reaction centers of *Rhodobacter spaeroides*, where native ubiquinone molecules can be reversibly removed from the Q_A site and functionally replaced with a variety of artificial quinones (*43*−*47*), extraction of plastoquinone from PS II and its replacement with other quinones has proven to be much more difficult (*8*, *48*). We propose here that the V247M/A249T double mutation in the Q_A binding pocket of the D2 protein makes the process of Q_A exchange with exogenous quinones possible under physiological conditions *in situ*. The concept of a mobile Q_A in the D2R8 mutant and, to a lesser extent, in the A249T strain explains the fluorescence data and is compatible with the observations that (1) the site of quinone action in the D2R8 mutant is not at the level of Q_B and (2) addition of artificial quinones influenced the charge recombination rate of Q_A^- and the donor side. According to this interpretation, the Q_A pocket in the D2R8 mutant therefore either can be empty, contain a PQ, or contain an artificial quinone that had been added. As in the presence of all artificial quinones tested except DQ the rate of fluorescence induction in the presence of DCMU was increased, artificial quinones (except DQ) at the

Q_A site in the mutant are able to accept an electron. However, if an artificial quinone functions as Q_A, the apparent $Q_A{\cdot}^- Q_B \rightleftharpoons Q_A{\cdot}Q_B^-$ equilibrium has shifted to the left in comparison with centers with PQ at the Q_A site: as shown in Figure 6, full Q_A^- oxidation is not obtained in the D2R8 mutant within 25 ms after a flash if an artificial quinone is present.

The shifted semiquinone equilibrium suggests an increased (more positive) E_m of the Q_A/Q_A^- couple in the D2R8 mutant if DCBQ is at the Q_A site as compared to when PQ is at the site. The charge recombination rate between Q_A^- and the donor side, however, is increased if DCBQ is added, which is indicative of a decreased stability of Q_A^- when DCBQ is at the site as compared to the situation when native PQ is present in the Q_A niche of the D2R8 mutant. This suggests that the charge recombination rate is not determined solely by thermodynamics, but that other factors such as the position and/or orientation of Q_A may contribute to the charge recombination rate as well. A similar conclusion has been reached using the H268Q mutant that lacks a functional non-heme iron (*7*).

In the presence of DQ, no electron transport to the Q_A site could be observed, and the quinone appears to be bound to the site as electron transfer is strongly inhibited at low DQ concentrations. As could be expected using the concept of a competitive binding of multiple quinones to the Q_A site, DQ inhibition of Q_A reduction is relieved by addition of excess DCBQ (data not shown). The question is why DQ cannot be reduced at the Q_A site. A thermodynamic limitation as a consequence of a decreased (more negative) quinone/semiquinone midpoint redox potential for DQ at the Q_A site is unlikely as the E_m for pheophytin reduction is -610 mV (*49*) and therefore the E_m of the Q_A/Q_A^- couple can drop by several hundreds of millivolts before electron transfer to Q_A becomes thermodynamically unfavorable. According to determinations of the E_m of the DQ/DQ^- couple in the Q_A site of isolated reaction centers from *Rhodobacter sphaeroides*, this value is expected to be very close to that of Q_A/Q_A^- in native reaction centers (*45*, *46*). Therefore, the presence of DQ in the Q_A site of PS II should not pose thermodynamic limitations on electron transfer from pheophytin to Q_A. A more likely explanation is a kinetic limitation of Q_A reduction if DQ is at the site. Reduced pheophytin has an increased probability to react with $P680^+$ instead of with Q_A if Q_A reduction kinetics have been slowed. An illustration of this phenomenon is the bacterial reaction center lacking the non-heme iron (*50*); in this system, the quantum yield of charge separation has been decreased by a factor of 2. In PS II, functional removal of the non-heme iron has a much larger effect on the quantum yield of Q_A reduction, reducing the quantum yield to only a few percent (*7*). The quantum yield of Q_A reduction in D2R8 with DQ at the Q_A site is likely to be even lower as complete inhibition of oxygen evolution by DQ at saturating light intensity is achieved at about 20 μM (Figure 1). As suggested by the decreased quantum yield of oxygen evolution in D2R8 in the absence of artificial quinones, the rate of Q_A reduction in this mutant with PQ at the site is also likely to be smaller than in the wild type.

An interesting feature of the D2R8 mutant is the slow fluorescence induction in the presence of DCMU and the absence of artificial quinones. This suggests that at the start of illumination in very few centers a functional Q_A is present, and that the number of centers with a functional Q_A increases with illumination time. Interestingly, in the A249T mutant after dark-adaptation in the absence of artificial quinones, about half of the centers possess a reducible Q_A whereas after a brief illumination essentially all centers contain functional Q_A. This suggests that in darkness the affinity of the Q_A site for PQ is significantly lower than in the light. Several explanations may be given for this phenomenon: One is that the semiquinone form has a higher affinity for the Q_A site than the quinone form. Precedence for this is provided by the Q_B site, where Q_B^- is tightly bound whereas the quinone and quinol forms are not. However, even if Q_A is in Q_A^- form half of the time, a much smaller difference in Q_A occupancy by PQ would be expected between darkness and light than the "all-or-none" phenomenon that is observed in the D2R8 mutant. Another explanation may be that the PQ affinity for the Q_A site in the light is intrinsically higher than in darkness, for example, because of conformational differences at the Q_A site in the mutant. It is likely that the latter explanation contributes significantly to the differences that are observed experimentally.

The reasoning of full occupancy of the Q_A site by PQ in the light in the absence of artificial quinones in the mutants studied here is in line with the results of oxygen evolution experiments: the D2R8 mutant as well as the A249T strain exhibit oxygen evolution yields that are proportional to the number of PS II centers measured by DCMU binding. Therefore, essentially all PS II centers are active under the steady-state illumination conditions of oxygen evolution measurements.

Alternate explanations to interpret the data are possible, but much less likely. One such explanation is that in the D2R8 mutant quinones would bind at a site different from that of Q_A, and compete functionally for electrons from reduced pheophytin. However, this is unlikely as electron transfer between pheophytin and Q_A is rapid (on the subnanosecond time scale in the wild type and presumably slightly slower in the mutant), and electron transfer to quinones bound at "unspecific" sites is not expected to be so fast to compete with this process.

Even though fluorescence induction measurements are valuable to monitor events that occur within several seconds, interpretation of changes that occur on a longer time scale is more difficult. The very slow and relatively small rise in the fluorescence yield in the D2R8 mutant in the absence of additions is due only partially to reduction of Q_A (Figure 3D). When turning off the light under these conditions, only a small part of the fluorescence yield (the part that is correlated directly with Q_A^-) drops rapidly, whereas the remainder of the fluorescence yield decays much more slowly. This is consistent with efficient electron transfer between Q_A and Q_B that is observed in the D2R8 mutant (Figure 6). Also in the PS II-less *psbDIC*$^-$/*psbDII*$^-$ mutant a small, slow rise in the variable fluorescence yield was observed on the time scale of 10 s (data not shown), which could be due to, for example, state transitions or pH changes in the surrounding medium.

Unfortunately, upon introduction of the D2R8 and A249T mutations into a PS I-less strain, PS II stability and/or synthesis/assembly seemed to have been impaired to a point where no PS II centers could be detected. This is the first

time that introduction of a mutation leading to a photoautotrophic phenotype in a PS I-containing strain leads to a loss of PS II centers in a PS I-less strain. In other instances, where mutations are mostly on the PS II donor side, the amount of PS II per cell in PS I-less strains is similar to or more than the amount in PS I-containing strains [for example,see (*17, 51*)]. The reasons for this striking difference are not yet clear.

The results presented in this paper indicate that relatively small changes in the primary structure of the Q_A binding environment have very significant effects on the properties of Q_A. The apparently efficient exchange of quinones at the Q_A site of the D2R8 mutant suggests that the Q_A site is relatively accessible. Therefore, the V247M and particularly the A249T mutations appear to have provided Q_A with selected properties of Q_B (i.e., exchange of the quinone in the site). However, thus far we have not obtained evidence that would be indicative of double-reduction of Q_A in any of the mutants, thus leaving one prominent characteristic of the wild-type Q_A site fully intact in the mutants.

REFERENCES

1. Michel, H., and Deisenhofer, J. (1988) *Biochemistry 27*, 1−7.
2. Diner, B. A., and Babcock, G. T. (1996) in *Oxygenic Photosynthesis: The Light Reactions* (Ort, D. R., and Yocum, C. F., Eds.) pp 213−247, Kluwer Academic Publishers, Dordrecht, The Netherlands.
3. Debus, R. J. (1992) *Biochim. Biophys. Acta 1102*, 269−352.
4. Britt, R. D. (1996) in *Oxygenic Photosynthesis: The Light Reactions* (Ort, D. R., and Yocum, C. F., Eds.) pp 137−164, Kluwer Academic Publishers, Dordrecht, The Netherlands.
5. Nitschke, W., and Dracheva, S. M. (1995) in *Anoxygenic Photosynthetic Bacteria* (Blankenship, R. E., Madigan, M. T., and Bauer, C. E., Eds.) pp 775−805, Kluwer Academic Publishers, Dordrecht, The Netherlands.
6. Svensson, B., Etchebest, C., Tuffery, P., van Kan, P., Smith, J., and Styring, S. (1996) *Biochemistry 35*, 14486−14502.
7. Vermaas, W., Vass, I., Eggers, B., and Styring, S. (1994) *Biochim. Biophys. Acta 1184*, 263−272.
8. Diner, B. A., de Vitry, C., and Popot, J.-L. (1988) *Biochim. Biophys. Acta 934*, 47−54.
9. Hankamer, B., Barber, J., and Boekema, E. J. (1997) *Annu. Rev. Plant Physiol. Plant Mol. Biol. 48*, 641−671.
10. Nagatsuka, T., Fukuhara, S., Akabori, K., and Toyoshima, Y. (1991) *Biochim. Biophys. Acta 1057*, 223−231.
11. Kitamura, K., Ozawa, S., Shiina, T., and Toyoshima, Y. (1994) *FEBS Lett. 354*, 113−116.
12. Ozawa, S., Kobayashi, T., Sugiyama, R., Hoshida, H., Shiina, T., and Toyoshima, Y. (1997) *Plant Mol. Biol. 34*, 151−161.
13. Zheng, M., and Dismukes, G. C. (1996) *Biochemistry 35*, 8955−8963.
14. Krieger, A., Rutherford, A. W., and Johnson, G. N. (1995) *Biochim. Biophys. Acta 1229*, 193−201.
15. Krieger, A., and Rutherford, A. W. (1997) *Biochim. Biophys. Acta 1319*, 91−98.
16. Miksovska, J., Maróti, P., Tandori, J., Schiffer, M., Hanson, D. K., and Sebban, P. (1996) *Biochemistry 35*, 15411−15417.
17. Ermakova-Gerdes, S., Shestakov, S., and Vermaas, W. (1996) *Plant Mol. Biol. 30*, 243−254.
18. Kless, H., and Vermaas, W. (1996) *Biochemistry 35*, 16458−16464.
19. Vermaas, W. F. J., Charité, J., and Eggers, B. (1990) in *Current Research in Photosynthesis* (Baltscheffsky, M., Ed.) Vol. 1, pp 231−238, Kluwer Academic Publishers, Dordrecht, The Netherlands.
20. Ermakova-Gerdes, S., Shestakov, S., and Vermaas, W. (1995) in *Photosynthesis: From Light to Biosphere* (Mathis, P., Ed.) Vol. 1, pp 483−486, Kluwer Academic Publishers, Dordrecht, The Netherlands.
21. Rippka, R., Deruelles, J., Waterbury, J. B., Herdman, M., and Stanier, R. Y. (1979) *J. Gen. Microbiol. 111*, 1−61.
22. Pine, R., and Huang, P. C. (1987) *Methods Enzymol. 154*, 415−430.
23. Shapiro, R., Braverman, B., Louis, J. B., and Servis, R. E. (1973) *J. Biol. Chem. 248*, 4060−4064.
24. He, Q., Brune, D., Nieman, R., and Vermaas, W. (1998) *Eur. J. Biochem. 253*, 161−172.
25. Vermaas, W. F. J., Charité, J., and Shen, G. (1990) *Biochemistry 29*, 5325−5332.
26. Kless, H., Oren-Shamir, M., Ohad, I., Edelman, M., and Vermaas, W. (1993) *Z. Naturforsch. 48C*, 185−190.
27. Vermaas, W. F. J., Shen, G., and Styring, S. (1994) *FEBS Lett. 337*, 103−108.
28. Vermaas, W. F. J., and Arntzen, C. J. (1983) *Biochim. Biophys. Acta 725*, 483−491.
29. Satoh, K., Oh-hashi, M., Kashino, Y., and Koike, H. (1995) *Plant Cell Physiol. 36*, 597−605.
30. Bittersmann, E., and Vermaas, W. F. J. (1991) *Biochim. Biophys. Acta 1098*, 105−116.
31. Pakrasi, H. B., and Vermaas, W. F. J. (1992) in *The Photosystems: Structure, Function, and Molecular Biology. Current Topics in Photosynthesis, Volume 11* (Barber, J., Ed.) pp 231−256, Elsevier, Amsterdam.
32. Michel, H., Epp, O., and Deisenhofer, J. (1986) *EMBO J. 5*, 2445−2451.
33. Allen, J. P., Feher, G., Yeates, T. O., Komiya, H., and Rees, D. C. (1988) *Proc. Natl. Acad. Sci. U.S.A. 85*, 8487−8491.
34. El-Kabbani, O., Chang, C.-H., Tiede, D., Norris, J., and Schiffer, M. (1991) *Biochemistry 30*, 5361−5369.
35. Atashkin, A. V., Kawamori, A., Kodera, Y., Kuroiwa, S., and Akabori, K. (1995) *J. Chem. Phys. 102*, 5583−5588.
36. Tang, X.-S., Peloquin, J. M., Lorigan, G. A., Britt, R. D., and Diner, B. A. (1995) in *Photosynthesis: From Light to Biosphere* (Mathis, P., Ed.) Vol. I, pp 775−778, Kluwer Academic Publishers, Dordrecht, The Netherlands.
37. Vermaas, W., Charité, J., and Shen, G. (1990) *Z. Naturforsch. 45C*, 359−365.
38. Johanningmeier, U., Bodner, U., and Wildner, G. F. (1987) *FEBS Lett. 211*, 221−224.
39. Perewoska, I., Etienne, A.-L., Miranda, T., and Kirilowsky, D. (1994) *Plant Physiol. 104*, 235−245.
40. Lardans, A., Gillham, N. W., and Boynton, J. E. (1997) *J. Biol. Chem. 272*, 210−216.
41. Trebst, A. (1986) *Z. Naturforsch. 41C*, 240−245.
42. Oettmeier, W., Masson, K., Höhfeld, J., Meyer, H., Pfister, K., and Fischer, H.-P. (1989) *Z. Naturforsch. 44C*, 444−449.
43. Cogdell, R. J., Brune D. C., and Clayton R. K. (1974) *FEBS Lett. 45*, 344−347.
44. Okamura, M. Y., Isaacson, R. A., and Feher, G. (1975) *Proc. Natl. Acad. Sci. U.S.A. 72*, 3491−3495.
45. Woodbury, N. W., Parson, W. W., Gunner, M. R., Prince, R. C., and Dutton, P. L. (1986) *Biochim. Biophys. Acta 851*, 6−22.
46. Gunner, M. R., Robertson, D. E., and Dutton, P. L. (1986) *J. Phys. Chem. 90*, 3783−3795.
47. Giangiacomo, K. M., and Dutton (1989) *Proc. Natl. Acad. Sci. U.S.A. 86*, 2658−2662.
48. Araga, C., Akabori, K., Sasaki, J., Maeda, A., Shiina, T., and Toyoshima, Y. (1993) *Biochim. Biophys. Acta 1142*, 36−42.
49. Rutherford, A. W., Mullet, J. E., and Crofts, A. R. (1981) *FEBS Lett. 123*, 235−237.
50. Kirmaier, C., Holten, D., Debus, R. J., Feher, G., and Okamura, M. Y. (1986) *Proc. Natl. Acad. Sci. U.S.A. 83*, 6407−6411.
51. Manna, P., LoBrutto, R., Eijckelhoff, C., Dekker, J. P., and Vermaas, W. (1998) *Eur. J. Biochem. 251*, 142−154.

BI9806596